NATURAL PRODUCT RESEARCH
https://doi.org/10.1080/14786419.2022.2095634

Taylor & Francis
Taylor & Francis Group

Check for updates

Non-sulfated steroidal glycosides cistoindosides from marine 'old woman octopus' *Cistopus indicus* attenuate pro-inflammatory lipoxygenase

Silpa Kunnappilly Paulose[a,b]* and Kajal Chakraborty[a]

[a]Central Marine Fisheries Research Institute, Cochin, Kerala, India; [b]Department of Chemistry, Mangalore University, Mangalagangothri, Karnataka, India

ABSTRACT

Two non-sulfated steroidal glycosides, cistoindosides A-B were isolated from organic extract of the marine 'old woman octopus' *Cistopus indicus* (family Octopodidae). Their structures were characterized as 3β-acteoxy-23β-hydroxy-cholesta-9-ene-β-D-xylopyranoside (cistoindoside A) and 22,23-epoxy-3β-hydroxy-cholesta-5-ene-β-D-4'-*O*-acetoxy-xylopyranoside (cistoindoside B). Cistoindoside B, glycosylated with β-D-4'-*O*-acetoxy-xylopyranoside in conjunction with epoxy moieties displayed superior anti-inflammatory properties as acknowledged by its promising 5-lipoxygenase attenuation potential (IC_{50} 2.11 μM) than the 5-lipoxygenase inhibitor drug zileuton (IC_{50} 3.76 μM). The anti-inflammatory properties were corroborated by the promising antioxidant activities (IC_{50} $\sim$ 1.0–1.5 mM) of these steroid glycosides. Sizeably greater electronic properties, balanced hydrophobic-lipophilic properties (log P_{OW} $\sim$ 4.0) and comparatively lower steric factors were directly proportional to their bioactivities. Molecular simulation studies in the active sites of 5-lipoxygenase displaying lesser binding energies and inhibition constant (K*i*) of cistoindoside B could be correlated with anti-inflammatory properties. Cistoindosides could be projected for their utilization as potential bioactive leads in functional food and pharmaceutical applications.

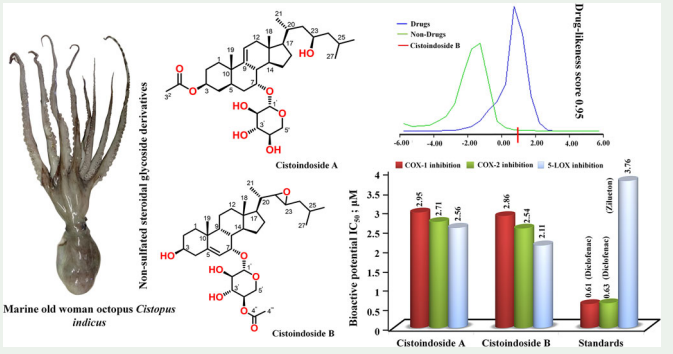

ARTICLE HISTORY

Received 20 March 2022
Accepted 19 June 2022

KEYWORDS

Marine octopus *Cistopus indicus*; Octopodidae; steroidal glycosides; cistoindosides A-B; inflammatory 5-lipoxygenase

CONTACT Kajal Chakraborty kajal_cmfri@yahoo.com

Supplemental data for this article can be accessed online at https://doi.org/10.1080/14786419.2022.2095634.

*Silpa Kunnappilly Paulose and Kajal Chakraborty contributed equally to this work.

© 2022 Informa UK Limited, trading as Taylor & Francis Group

1. Introduction

Steroidal glycosides form a significant chemical class of natural products having both terrestrial and marine origin. Previously, the steroidal oligosaccharides were considered as common secondary metabolites of higher plants, nevertheless over the past six decades there has been rapidly growing interests towards the steroidal glycosides from marine invertebrates by reason of their exceptional structural diversities and varied biological potentials (Ivanchina et al. 2011). Most of the steroidal glycoside compounds are cytotoxic, and exhibited profound antibacterial, anti-tumour, hypo-cholesterolemic, and other biological activities owing to their considerable glycosylation to lipophilic membrane bound free sterols (Francis et al. 2002, Grille et al. 2010). Steroidal glycosides possess sugar moieties at the 3-hydroxy/acetoxy group, other hydroxyl positions, or at the side chain of a reformed sterol framework (Grille et al. 2010). Common monosaccharides identified in marine steroidal glycosides include galactose, glucose, xylose, and arabinose in addition to amino-sugars/deoxy groups/sulfated and/or methylated sugars, wherein the monosaccharide units form both furanose and pyranose forms in the glycosidal part (Ivanchina et al. 2011). Previous publications described the presence of cytotoxic steroidal glycosides from a gastropod mollusc *Conus pulicarius* (Lee et al. 2017). Another series of steroidal glycosides with xylose monosaccharide units together with two new pentaceroside metabolites identified from the starfish *Pentaceraster gracilis* were reported to possess activities against various human cancer cell lines (Vien et al. 2017). These diverse metabolites were synthesized as a part of defense mechanism through complex biochemical and physiological mechanisms when subjected to competitive and hostile conditions of extreme temperatures, microbial infections and salinity of the benthic locations of the sea (Pati et al. 2015).

Cephalopod mollusc has been acknowledged as high-value nutritional food source and culinary delicacies, especially in the Asian countries attributable to high economic value (Nichols et al. 1998). The presently studied marine 'old-woman octopus', *Cistopus indicus* (Rapp [in Férussac & d'Orbigny], 1835) is ubiquitous in the tropical Indian Ocean and South Pacific waters (Dou et al. 2020). Earlier literatures reported various pharmacological activities, such as anti-inflammatory, anti-oxidative, anti-hypertensive, and anti-diabetic properties from cephalopoda molluscs (Krishnan and Chakraborty 2019; Krishnan et al. 2020), and reports of secondary metabolites including bislactonic macrodiolides from the studied marine octopus (Paulose and Chakraborty 2021; 2022) comprehended the importance of the current work. Thus, in continuation with our ongoing search for structurally diverse and biologically active secondary metabolites from *C. indicus* collected from the Southwestern coast of the Arabian Sea resulted in the identification of two steroidal glycosides cistoindosides A-B from the organic extract by repetitive chromatographic fractionation. Pharmacological activities were assessed using various *in vitro* antioxidant {2,2-diphenyl-1-picrylhydrazyl and 2,2′-azino-bis (3-ethyl benzothiazoline-6-sulphonic acid ($ABTS^{+}$) radical scavenging} and anti-inflammatory {cycloxygenase 1 and 2 (COX-1/2), 5-lipoxygenase (5-LOX)} assays, and the results were compared against various commercial standards. Various physicochemical parameters (electronic, steric and other molecular descriptors) were related with the structural features displaying bioactivities. *In silico* molecular docking studies

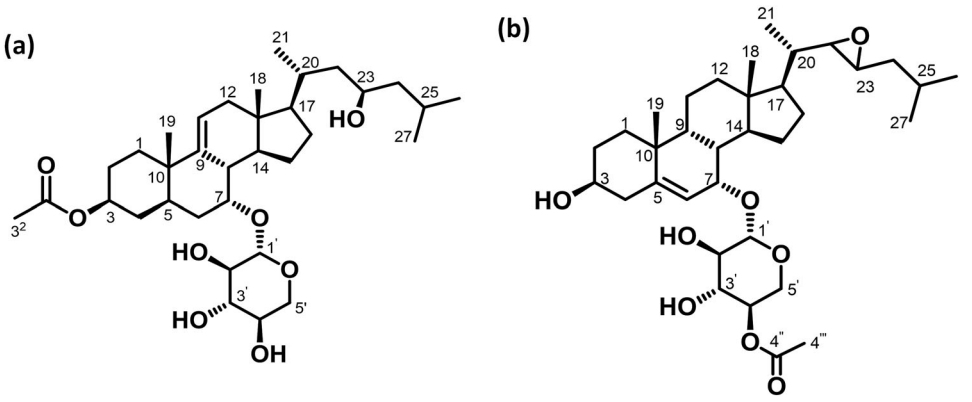

Figure 1. Structural representations of non-sulfated steroidal glycoside analogues, (a) cistoindoside A and (b) cistoindoside B purified from the organic extract of *Cistopus indicus*.

of titled compounds (cistoindosides A-B) with 5-LOX corroborated its mode of inhibition by interactions in the active sites of the enzyme.

2. Results and discussion

2.1. Bioactivity-piloted chromatographic fractionation of cistoindosides from C. indicus

The ethyl acetate:methanol (EA: MeOH) extract of *C. indicus* was repetitively fractionated by exhaustive chromatographic techniques. Initial separation of the crude was performed using size exclusion gel permeation chromatographic method over a lipophilic (LH-20) sephadex stationary phase equilibrated with HPLC grade methanol to yield seven fractions, which were combined to four groups (Cl_a-Cl_d) after TLC (*n*-hexane:EA, 7:3, and dichloromethane DCM:MeOH, 9:2, 7:3, 1:1 v/v) and HPLC experiments over a reverse-phase octadecylsilane stationary phase (RPC_{18}, MeOH:acetonitrile ACN, 1:1, v/v). The Cl_b sub fraction displaying greater bioactivities among other fractions was selected for further purification on a pressurized liquid column (flash chromatography) filled with 230–400 mesh sized silica gel using *n*-hexane/EA/MeOH to obtain 5 fractions, which were reduced to four ($Cl_{b\text{-}1}$ through $Cl_{b\text{-}4}$). Among these fractions, $Cl_{b\text{-}3}$ registered greater bioactivities, and thus, was selected for further purification on preparative reverse phase (RPC_{18}, 5 μm) HPLC with MeOH: ACN (1:1, v/v) eluent system to afford two homogenous compounds (after HPLC over RPC_{18} stationary phase, MeOH:acetonitrile ACN, 1:1, v/v), which were characterized as 3β-acteoxy-23β-hydroxy-cholesta-9-ene-β-D-xylopyranoside (cistoindoside A) and 22,23-epoxy-3β-hydroxy-cholesta-5-ene-β-D-4′-*O*-acetoxy-xylopyranoside (cistoindoside B) (Figure 1).

2.2. Spectroscopic characterization

2.2.1. Cistoindoside A

The molecular formula of the isolated steroidal glycoside derivative cistoindoside A was deduced as $C_{34}H_{56}O_8$ (high-resolution electrospray ionization mass spectrum,

HRESIMS *m/z* 593.4057 $[M+H]^+$), and the structure was elucidated as 3β-acteoxy-23β-hydroxy-cholesta-9-ene-β-D-xylopyranoside, based on detailed NMR, mass spectral and FTIR data (Table S2, Figures S1–S12). Seven degrees of unsaturation corresponding to one each of olefinic and carbonyl along with five ring systems of characteristic tetracyclic nucleus of cholesterol including a monosaccharide sugar moiety were perceived. The ^{13}C NMR spectrum along with distortionless enhancement by polarization transfer DEPT-135 (Figures S2–S3) displayed the resonances for 34 carbon atoms, which comprised of four quaternary carbons, ten methylenes, six methyls, and fourteen methines (including one olefinic methine and four oxymethines). The characteristic ^{13}C NMR signal appeared at δ_C 170.5 was allocated to the carbonyl carbon of ester functionality. Detailed examination of one and two-dimensional NMR spectroscopic data attributed the presence of cholesterol moiety except for some additional resonance peaks and differences in the chemical shift values corresponding to the side chain substitution in the core (Fang et al. 2013). The considerably deshielded singlet methyl protons at δ_H 2.02 (H-3^2) displayed HMBC cross-peaks with the carbonyl carbon at δ_C 170.5 that supported that it might be an acteoxy group. Further long range HMBC couplings from δ_C 170.5 (C-3^1) to the considerably downshifted methine proton at δ_H 3.80 (H-3) confirmed the presence of acetoxy functionality at C-3 position of cistoindoside A. The ^{1}H-^{1}H correlation spectroscopy (COSY) identified four isolated spin systems (A-D), which suggested partial structural framework of the titled compound (Figure S4). The presence of a sugar moiety was identified via anomeric carbon signal at δ_C 104.8 exhibiting heteronuclear single quantum correlation (HSQC) relation with the anomeric proton signal at δ_H 5.02 (H-1′). Careful interpretation of the HSQC, HMBC, COSY, and TOCSY spectral data led to assignment of saccharide moiety (Table S1). The long range HMBCs of the anomeric proton H-1′ (δ_H 5.02) with C-7 (δ_C 86.3) and C-2′ (δ_C 73.5) substantiated the position of inter-glycosidic linkage and attachment of the sugar chain at C-7 of the studied steroid derivative. These assignments were in agreement with previously reported steroidal glycoside from gastropod mollusc (Lee et al. 2017). The COSY spin system, **D**; δ_H 5.02 (H-1′)/δ_H 3.70 (H-2′)/δ_H 3.50 (H-3′)/δ_H 3.41 (H-4′)/δ_H 4.07 (H-5′) was found to be enclosed in the saccharide unit linked via electronegative oxygen atom to the C-7 position of the tetracyclic steroid core considered as characteristic COSY correlation of a pyranoside monosaccharide moiety (Fang et al. 2013). The interchangeable hydroxyl protons at δ_C 66.0 (C-23) were ceased to exist upon interchange of D_2O, asserting the presence of hydroxyl group in its vicinity. The one bond ^{1}H-^{1}H COSY spin system **C**; δ_H 1.48 (H-22)/δ_H 3.20 (H-23)/δ_H 1.45 (H-24)/δ_H 1.69 (H-25)/δ_H 0.94 (H-27) was recorded within the 2-methyl heptanol branching. Significantly deshielded ^{13}C NMR resonance at δ_C 115.4 (C-11) and quaternary signal at δ_C 145.7 (C-9) indicated that the olefinic position has been shifted to C-9 from the basic cholesterol, which was further confirmed by HMBC couplings from δ_H 5.32 (H-11) to δ_C 44.6 (C-12) and δ_H 1.98 (H-12) to δ_C 145.7 (C-9). The partial structure of sugar moiety was accomplished by COSY and HMBC spectra. The COSY correlations (spin system **D**); δ_H 5.02 (H-1′)/δ_H 3.70 (H-2′)/δ_H 3.50 (H-3′)/δ_H 3.41 (H-4′)/δ_H 4.07 (H-5′) was linked via electronegative oxygen atom to the C-7 position implied a 6-deoxyhexose unit. The large coupling constant of the anomeric proton δ_H 5.02 (H-1′, d, $J = 7.6$ Hz) confirmed it as an axial proton (β-orientation), which was joined to C-7 from the

HMBC correlations between δ_H 5.02 (H-1′) to δ_C 86.3 (C-7), and thus, was attributed to be β-oriented. NOESY correlations were also observed between anomeric H-1′ and H-3′ protons, indicating a diaxial relationship between the protons, and thus, the glycosyl moiety was attributed to β-D-xylose. Also, the optical rotation value of the hydrolyzed product (+ 18.5) was in good agreement with the reference D-xylose (+18.6), which also supported the configuration of the sugar moiety as D-xylose. These attributions were in accordance with the reported steroidal glycosides from the marine gastropod snail *Conus pulicarius* (Lee et al. 2017). The relative configuration of chiral centres of basic cholesterol moiety was deduced based on previous works of literature and nuclear overhauser effect spectroscopy (NOESY) correlation experiments (Figure S8). NOESY correlations δ_H 3.80 (H-3) with δ_H 3.41 (H-4′) and δ_H 1.57 (H-5), and further with δ_H 3.70 (H-2′) accredited that these protons were disposed in the direction of the same plane of reference. An earlier literature (Lee et al. 2017) reported that the H-3 proton in the basic cholesterol nucleus were in α-orientation, and hence, these protons could be arbitrarily assigned as α-oriented. Other NOE cross-peaks recorded between the protons at δ_H 5.02 (H-1′)/3.50 (H-3′); δ_H 2.74 (H-7)/δ_H 2.32 (H-8)/δ_H 1.36 (H-19) acknowledged their spatial proximity, and were aligned in same plane of symmetry (β-protons), and oppositely oriented to the α-protons. These assignments were in accordance with earlier literature reports (Lee et al. 2017). The molecular ion peak of the isolated cistoindoside A was recorded at *m/z* 592 (Figures S10–S11). The fragmentation involving McLafferty rearrangement of the titled compound led to the elimination of acteoxy group to yield a fragment at *m/z* 532 (b). The mass fragmentation pathways attributed the base peak at *m/z* 59 corresponding to an acetoxy fragment. The IR spectrum recorded stretching absorptions at 3427 and 1733 cm^{-1}, which correspond to the hydroxyl and ester carbonyls functionalities, respectively in the studied compound.

2.2.2. Cistoindoside B

The molecular formula of cistoindoside B was deduced as $C_{34}H_{54}O_8$ (HRESIMS *m/z* 591.3901 $[M+H]^+$), and the structure was elucidated as 22,23-epoxy-3β-hydroxy-cholesta-5-ene-β-D-4′-*O*-acetoxy-xylopyranoside, based on detailed NMR, mass spectral and FTIR data (Table S2, Figures S15–S26). The double bond equivalence was calculated as eight, which included two unsaturations of olefinic and carbonyl and six ring moieties. Detailed interpretation of the ^{1}H and ^{13}C NMR spectral data implied that cistoindoside B shared similar tetracyclic carbon framework as that of its A analogue, except for few changes in the chemical shift values in the NMR spectra (Table S2; Figure 1; Figure S29). The ^{13}C NMR data for the substituted glycosidal residue at C-7 position of tetracyclic core nucleus of cistoindoside B at δ_C 105.4 (C-1′), 76.4 (C-2′), 66.2 (C-3′), 72.5 (C-4′), and 61.1 (C-5′) were in good agreement with those of cistoindoside A at δ_C 104.8 (C-1′), 73.5 (C-2′), 76.6 (C-3′), 70.7 (C-4′), and 63.0 (C-5′) except for an additional acetyl substitution including a carbonyl peak at δ_C 172.2 at C-4′′ position (Figure S16), thereby attributing the presence of an *O*-acetyl derivative of xylopyranose compared to cistoindoside A. The arrangements with the spin-coupling array of the sugar proton signals were indicative for a β-D form of xylose (Lee et al. 2017). Comparatively lesser deshielded proton resonance at δ_H 3.20 (H-3) with A analogue δ_H

3.80 (H-3) implying the presence of a hydroxyl group at C-3 position instead of an acetoxy entity, which was further confirmed with the absence of long-range couplings with the carbonyl group exhibited by cistoindoside A. The ^{13}C-NMR chemical shift of C-3 at δ_C 71.4 is indicative of a carbon possessing a α-oriented proton (Ngoc et al. 2017). The configuration of the hydroxyl group at C-3 position of the titled compound was determined as β-oriented in comparison with the similar carbon signal at C-3 (δ_C 70.7) of cistoindoside B with 3β-hydroxycholest-5-en-7-one (δ_C 71.4), which is quite different from that of 3α-OH carbon (aragusterol G) with carbon signal at δ_C 66.4 (Mitome et al. 2003). Thus, the configuration of C-OH was attributed to β-oriented. The proton signal appeared at downfield region δ_H 5.26 (H-6) attached to an olefinic carbon δ_C 126.2 (HSQC, Figure S20) being typical of the endocyclic olefinic proton at C-6 position in the Δ^5 sterols reported from molluscan species (Salas and Chakraborty 2018). The lesser deshielded signals appeared in the ^{13}C NMR spectrum (C-22 at δ_C 66.0 and C-23 at δ_C 56.2) and in ^{1}H NMR spectrum (H-22 at δ_H 2.54 and H-23 at δ_H 2.58) were attributed to the epoxide signals on comparison with earlier reported literature (Funel et al. 2004). Further, the *trans* relationship of the H-22 and H-23 protons was unambiguously determined by the coupling constant of 2.2 Hz (Funel et al. 2004). The relative stereochemistry of the chiral centers was assigned based on the nuclear overhauser effect spectroscopy (NOE, Figure S22) and coupling constants, which were also comparable with the A analogue. The NOE spatial correlation between δ_H 3.20 (H-3)/δ_H 3.75 (H-2′)/δ_H 4.19 (H-4′)/δ_H 1.44 (H-9)/δ_H 1.40 (H-14) δ_H 1.48 (H-17)/δ_H 2.58 (H-23) indicated that these protons were disposed at the same plane of the molecule and attributed to α-orientation. Similarly, the NOE cross-peaks between the proton sets δ_H 3.49 (H-3′)/δ_H 5.04 (H-1′)/δ_H 3.27 (H-7)/δ_H 1.71 (H-8)/δ_H 1.30 (H-19)/δ_H 1.94 (H-20)/δ_H 2.54 (H-22), which neither exhibited the correlation with α-set protons, was confirmed to be aligned in a plane opposite to the α-orientation, and was assigned as β-oriented. The molecular ion peak at *m/z* 590 {GC(EI)MS} (Figures S24–S25) together with 1 D and 2 D spectroscopic data assigned the molecular formula as $C_{34}H_{54}O_8$, with seven degrees of unsaturation. With two unsaturated system belongs to the olefinic and carbonyl residues deduced from the ^{13}C NMR experiment, the remaining unsaturations were accounted for the cyclic systems. The mass fragmentation could proceed via elimination of hydroxyl group from C-3 position and the side chain entity C_8H_{15} at C-17 position. The peak at *m/z* 192 was due to the removal of the glycosidal residue from the C-7 position. The base peak was obtained at *m/z* 80 corresponding to the cyclo-hexa-1,4 diene moiety.

2.3. Bioactivities of cistoindosides A-B isolated from C. indicus

Among the two isolated steroidal glycosides, the bioactivities of cistoindoside B were observed to be noticeably greater as compared to cistoindoside A. Cistoindoside B displayed considerably superior ($p < 0.05$) ABTS/DPPH radical quenching activities ($IC_{50} \sim$ 1.0–1.4 mM) as well as attenuating the pro-inflammatory enzymes COX-2 and 5-LOX (IC_{50} 2.0-3.0 μM) when compared to cistoindoside A (Table S3). Conspicuously, the 5-LOX attenuation property of cistoindoside B was significantly higher (IC_{50} 2.11 μM) than that showed by cistoindoside A (IC_{50} 2.56 μM) and standard anti-inflammatory

drug zilueton (IC_{50} 3.76 μM, $p < 0.05$). Earlier report of literature displayed that steroidal glycoside derivatives might be accountable towards anti-inflammatory potential (Fang et al. 2013). Perceptibly, the selectivity index (anti-COX-1/anti-COX-2) of cistoindosides A-B were found to be greater (>1) than the commercial drug diclofenac (0.96), which could corroborate to the promising anti-inflammatory properties. The anti-oxidant properties of the isolated metabolites were considerably higher than the reference standard α-tocopherol. Promising anti-oxidant property for cistoindoside B could possibly substantiate its attenuation potential against pro-inflammatory enzymes COX-1/2 and 5-LOX causing inflammatory disorders. The prospective anti-inflammatory activity of cistoindosides A-B might be due to the presence of electronegative moieties such as ester, hydroxyl, olefinic groups, which could be responsible for the dissociation of hydrogen atom from arachidonic acid, and also could fit well into the 5-LOX binding site regulating the production of pro-inflammatory leukotrienes and prostaglandins (Maneesh and Chakraborty 2017). These results inferred that the titled derivatives could form a valuable pharmacophore leads in future biomedical research to combat inflammatory ailments.

2.4. Structure activity relationship studies

Anti-oxidant and anti-inflammatory activities of cistoindosides A-B were corroborated with their physiochemical parameters (Antony and Chakraborty 2020a) (Table S3). Hydrophobicity factors appeared to play key functional characters towards their bioactivities. Particularly, a compound with lesser log P_{ow} (<5) was deliberated to be effective to sustain a desirable hydrophobic lipophilic balance (Lipinski and Hopkins 2004). The steroidal glycoside derivative, cistoindosides A (log P_{ow} 4.02) and B (log P_{ow} 3.91) exhibited preferred hydrophobic- lipophilic equilibrium (log P_{ow} 1–5) (Table S3). The comparable bulk (steric) parameters of cistoindosides (MR 150–160 cm^3/mol; MV 480-500 cm^3; Pr ∼ 1300 cm^3) with standard α-tocopherol might also add towards their greater antioxidant activities (Table S3). Likewise, the electronic properties of the cistoindosides (as determined by topological polar surface area) were considerably greater (tPSA > 100) as compared to those recorded with reference standards zilueton (tPSA 66.56), diclofenac (tPSA 49.33) and α-tocopherol (tPSA 29.46). Along with that the maximum electrophilic super delocalizability (SEMX 2.0-5.0), total absolute sigma charge (TCSH ∼5) and molecular polarizability (MPOL ∼60-65) of cistoindosides A-B were considerably greater than those exhibited by standard drugs (DPOL 2-3, SEMX 0-4, and MPOL 20-50), thus attributing the comparatively greater bioactivities of the studied compounds.

2.5. In silico molecular docking analysis of cistoindosides and drug-likeness

The molecular docking studies of cistoindosides A-B were performed against pro-inflammatory inducible 5-LOX enzymes (Table S4), which revealed that the docked ligands might potentially bind with the targets, and exhibited lowest binding energies ranging from −10.80 to −11.18 kcal/mol along with lowest docking scores of −9.73 to −12.14 kcal/mol. Notably, the lesser intermolecular energies −11.53 to −12.22 of

cistoindosides also could contribute to greater interaction in the active site of the 5-LOX enzyme. The cistoindosides A-B analogues further demonstrated three hydrogen bonding interactions in the active pocket, whereas, standard drug zilueton demonstrated only two (Figure S33). Greater number of hydrogen bonds of cistoindosides A-B in the active site of 5-LOX coupled with lesser docking parameters were found to be consistent with the greater bioactive potentials of the former as deduced from *in vitro* 5-LOX inhibitory assay (IC_{50} 2.11 μM). These attributions were further corroborated by greater drug-like attribute of cistoindoside B (drug-likeness score of 0.95) than A analogue (drug-likeness score of 0.80) (Figure S33), and therefore, could be a anticipated as prospective anti-inflammatory lead.

2.6. Biogenesis of cistoindosides

The biological function of steroid glycosides in marine animals involves in defence and reproductive processes (Makarieva et al. 1993). It was assumed that the precursor for the steroidal glycosides might be a membrane-bound free cholesterol molecule. A hypothetical biosynthetic pathway for cistoindoside A involves a hydroxylation at C-23 to yield 23-hydroxy cholesterol, which could isomerize and undergo hydrogenation at C9-C10 to yield 9-10-dihydro-23-hydroxy cholesterol. The epoxidation of the latter at C6-C7 position (by the epoxidase) could possibly lead to the formation of an unstable ergosterol epoxide, called as 6,7-epoxy-9, 10-dihydrocholesterol, which could undergo epoxide ring opening in a *trans*-diaxial fashion placing the hydroxyl at the C-7 position with minimal steric strain. It is observed that acetylation forms an integrated part for the biosynthesis of the steroid glycosides. Acetylation at C-3 position followed by *O*-linked glycosylation at C-7 could yield 3β-acteoxy-23β-hydroxy-cholesta-9-ene-β-D-xylopyranoside (cistoindoside A) (Figure S34). However, the first step for the biogenesis for 22,23-epoxy-3-hydroxy-cholesta-5-ene-β-D-4′-*O*-acetoxy- xylopyranoside involves the hydrogenation at C-22,23 of the precursor, cholesterol to form 22,23-dihydrocholesterol, followed by epoxidation to yield 22,23-epoxy cholesterol, which upon hydroxylation at C-3 position formed 22,23-epoxy-3-hydroxy-cholesterol. The latter could be subjected to glycosylation (by glycosyl transferase enzyme) to yield 22,23-epoxy-3-hydroxy-cholesta-5-ene-β-D-4′-*O*-acetoxy-xylopyranoside (cistoindoside B) (Figure S34).

3. Experimental

3.1. Chemicals, reagents, and instrumentation

Analytical/HPLC-grade solvents and reagents were used in this study (Sigma-Aldrich Chemical Co. Inc., MO, USA; E-Merck, Darmstadt, Germany). The instrumentation details were provided in the supplemental material S1.

3.2. Preparation of organic extract and chromatographic purification of cistoindoside A-B from C. indicus

The study material of *C. indicus* (Rapp, 1835) (Ferussac and d'Orbigny, 1834–1848) (Norman et al. 2014) (family Octopodidea) (∼5 kg, wet weight) (voucher specimen

number of CMFRI/DE.3.1.1/MBRM) were obtained from the south-western coastline of the Arabian Sea (Lat 8°48′ N; Long 78°9′ E and Lat 9°14′ N; Long 79°14′E) of the peninsular India during the month of February 2019. The samples were thoroughly cleaned with distilled water to eliminate the sand particles, mucus, and ink before being homogenized, and freeze dried by lyophilisation (Martin Christ alpha 1–4 LD Plus freeze-drier, Germany). The lyophilized residue (1250 g) was sonicated with ethyl acetate-methanol (EA: MeOH, 1:1 v/v; 1500 mL × 3) for 8 h, and later refluxed with EA: MeOH (1:1 v/v; 1500 mL × 3) at about 55 °C for 4 h under an inert N_2 atmosphere. The organic extract was dehydrated (over Na_2SO_4, ∼100 g) and concentrated by using a rotary vacuum evaporator (below 50 °C) (Heidolph, Germany) to result into a viscous residue, termed as crude organic extract of *C. indicus*. The extraction was repeated thrice to yield an amount of 55.3 g of crude (yield based on dry weight 4.42%). The extract of *C. indicus* (∼50 g) was chromatographically fractionated over cross-linked dextran-based resin (lipophilic Sephadex® LH-20, E-Merck, Germany) stationary phase (25–100 μm, 800 g) filled into a glass column (100 cm × 4 cm), with HPLC grade methanol. The various column fractions were combined to four (Cl_a through Cl_d) (Table S1) based upon TLC (DCM:MeOH, 9:2 v/v) and RP-C18 HPLC (ACN:MeOH, 50:50 v/v). The fraction Cl_b showed superior inhibition potential against 5-LOX/COX-2 coupled with DPPH/$ABTS^+$ scavenging property as compared to others (Table S1), and consequently, the fraction Cl_b was selected for further downstream purification on a silica gel (230–400 mesh). Gradient elution with *n*-hexane/EA/MeOH brought forth four pooled sub-fractions ($Cl_{b\text{-}1}$ through $Cl_{b\text{-}4}$). The fraction $Cl_{b\text{-}3}$ showed prospective bioactivities (Table S1), and thus, the fraction was purified using RP-C18 HPLC (MeOH:ACN, 50:50 v/v) to yield cistoindoside A (97 mg, and cistoindoside B (90 mg), and their purities were substantiated by TLC (DCM:MeOH, 9:2, v/v) and RP-C18 HPLC (MeOH:ACN, 1:1, v/v) experiments.

3.3. Spectroscopic analysis

3.3.1. Cistoindoside A

White amorphous solid; $[\alpha]^D_{26}$ −68.2 (MeOH, c0.014); m.p. 165-171 °C (decom.); TLC (silica gel GF254; dichloromethane (DCM): MeOH, 9:2, v/v) R_f: 0.32; ^{1}H NMR $_{MeOD}$ (500 MHz, δ_H in ppm, *J* in Hz) (Figure S1); ^{13}C NMR $_{MeOD}$ (125 MHz, δ_C in ppm) (Figure S2) ^{135}DEPT, ^{1}H-^{1}H COSY, TOCSY, HSQC, HMBC, NOESY data (Figures S3–S8, Table S2); HRMS (ESI): found *m/z* 593.4057 $[M+H]^+$, cal. for $C_{34}H_{57}O_8^+$ 593.4053 (Δ = 0.67 ppm) (Figure S9); GC-MS (EI): found *m/z* 592.4 $[M]^+$, cal. for $C_{34}H_{56}O_8$ (Figures S10–S11); FT-IR (stretching ν, bending δ, rocking ρ) (ν_{max}, cm^{-1}): 898.10 (alkene C-H_δ), 1049.05 (C-O-C_ν), 1469.20 (C-H_ρ), 2962.58 (C-H_ν), 1733.98 (C=O_ν), 3427.40 (OH_ν) (Figure S12); R_t (C_{18}-RP; MeOH-ACN, 50:50 v/v): 5.95 min (Figure S16); UV (MeOH) λ_{max} (log ε 3.59): 306 nm (Figure S14).

3.3.2. Cistoindoside B

White amorphous solid; $[\alpha]^D_{26}$ −72.5 (MeOH, c0.027); m.p. 175-179 °C (decom.); TLC (silica gel GF254; dichloromethane (DCM): MeOH, 9:2, v/v) R_f: 0.30; ^{1}H NMR $_{MeOD}$ (500 MHz, δ_H in ppm, *J* in Hz) (Figure S15); ^{13}C NMR $_{MeOD}$ (125 MHz, δ_C in ppm) (Figure

S16) ^{135}DEPT, ^{1}H-^{1}H COSY, TOCSY, HSQC, HMBC, NOESY data (Figures S17–S22, Table S2); HRMS (ESI): found *m/z* 591.3901 $[M+H]^+$, cal. for $C_{34}H_{55}O_8^+$ 591.3897(Δ = 0.69 ppm) (Figure S23); GC-MS (EI): found *m/z* 590.3 $[M]^+$, cal. for $C_{34}H_{54}O_8$ (Figures S24–S25); FT-IR (stretching ν, bending δ, rocking ρ) (ν_{max}, cm^{-1}): 896.91 (alkene C-H_δ), 1045.85 (C-O-C_ν), 1468.73 (C-H_ρ), 2926.31, 2852.76 (C-H_ν), 1731.52 (C = O_ν), 3440.36 (OH_ν) (Figure S26); R_t (C_{18}-RP; MeOH-ACN, 50:50 v/v): 5.58 min (Figure S27); UV (MeOH) λ_{max} (log ε 3.59): 286 nm (Figure S28).

3.4. Bioactivities of cistoindosides A-B and molecular docking analysis

Anti-inflammatory activities of studied non-sulfated steroidal glycosides, cistoindosides A-B and column sub-fractions fractionated from the solvent extract of *C. indicus* were examined by their inhibition potential against COX-1/2 (Larsen et al. 1996) and 5-LOX (Baylac and Racine 2003). Selectivity index (SI) with regard to anti-inflammatory properties was designed as the ratio of the attenuation property of cistoindosides against COX-1 to that against COX-2 (COX-1 inhibitory IC_{50}/COX-2 inhibitory IC_{50}) (Antony and Chakraborty 2020b). Antioxidant properties were assessed by the assays against stable DPPH and $ABTS^+$ radicals (Wojdylo et al. 2007), wherein the results of inhibition properties against the enzymes and oxidants (free radicals) were tabulated, and expressed in IC_{50} (concentration of samples at that they inhibit 50% of radical/enzyme activities; mg mL^{-1}/mM/μM) values. Structure-activity relationship studies were directed with molecular descriptors, for example hydrophobic (octanol-water partition coefficient/log P_{ow}), polar/electronic (topological polar surface area/tPSA, polarizability/PI), and bulk/steric (molar volume/MV, molar refractivity/MR, parachor/P) descriptors using ChemDraw Ultra (Cambridge Soft Corporation, USA; version 12.0) and ACD ChemSketch (version 2019.1; Advance Chemistry Development, Inc., Toronto, Canada). Molecular docking with 5-LOX was carried out by AutoDock 4 (AutoDock Tools version-1.5.6) with the crystal structure of the target protein (PDB ID 3v99; resolution 2.25 Å) (supplemental material S2) (Gilbert et al. 2012).

3.5. Statistical analysis

Statistical Program for Social Sciences 13.0 (SPSS Inc, Chicago, USA, version 13.0) was used to perform the statistical calculations. Analyses were performed in triplicate and the significant means of all parameters were examined by analysis of variance (ANOVA). The level of significance for all analyses was $p < 0.05$.

4. Conclusion

Two undescribed non-sulfated steroidal glycoside derivatives, called as cistoindoside A and B, with promising anti-inflammatory properties, were purified by bioactivity-assisted chromatographic fractionation of the organic extract of marine 'old women octopus' *C. indicus*. Cistoindoside B showed significant inhibition against pro-inflammatory 5-LOX (IC_{50} 2.11 μM) greater than standard drug zileuton (IC_{50} 3.76 μM). Similarly, the compound could efficiently attenuate COX-2 enzyme over COX-1 thus depicting

an acceptable anti-inflammatory selectivity index. These steroid glycoside derivatives also exhibited comparable antioxidant activities (IC_{50} 1.0–1.5 mM) to the commercial standard α-tocopherol (IC_{50} 1.5–1.8 mM). These results showed that cistoindoside B could be developed as a promising therapeutic lead against inflammatory diseases.

Funding and acknowledgements

The authors gratefully acknowledge the funding by the Indian Council of Agricultural Research (ICAR, New Delhi, India) under Central Marine Fisheries Research Institute (ICAR-CMFRI) project "Characterisation and evaluation of bioactive compounds from marine organisms for use against different diseases" (MBT/HM/SUB/23). The authors thank the Director, Indian Council of Agricultural Research-Central Marine Fisheries Research Institute (ICAR-CMFRI), and Head, Marine Biotechnology Division, ICAR-CMFRI for facilitating the research. The authors are thankful to the Chairman, Department of Chemistry, Mangalore University (Karnataka State, India) for providing with guidance and necessary support. S.K.P. gratefully acknowledges the Indian Council of Agricultural Research for financial support.

Disclosure statement

No potential conflicts of interest were reported by the authors.

Data availability

Chromatographic and spectroscopic spectral data are included as supplementary information.

References

Antony T, Chakraborty K. 2020a. First report of antioxidative *2H*-chromenyl derivatives from the intertidal red seaweed *Gracilaria salicornia* as potential anti-inflammatory agents. Nat Prod Res. 34(24):3470–3482.

Antony T, Chakraborty K. 2020b. First report of antioxidant abeo-labdane type diterpenoid from intertidal red seaweed *Gracilaria salicornia* with 5-lipoxygenase inhibitory potential. Nat Prod Res. 34(10):1409–1416.

Baylac S, Racine P. 2003. Inhibition of 5-lipoxygenase by essential oils and other natural fragment extracts. Int J Aromather. 13(2-3):138–142.

Dou C, Muhammad F, Liu L, Gong L, Chen Y, Guo B, Lü Z. 2020. Population diversity of *Cistopus indicus* inferred from mitochondrial DNA (cytochrome b) variation from China and Vietnam. Molluscan Res. 40(1):1–7.

Fang H-Y, Hsu C-H, Chao C-H, Wen Z-H, Wu Y-C, Dai C-F, Sheu J-H. 2013. Cytotoxic and anti-inflammatory metabolites from the soft coral *Scleronephthya gracillimum*. Mar Drugs. 11(6): 1853–1865.

Francis G, Kerem Z, Makkar HP, Becker K. 2002. The biological action of saponins in animal systems: a review. Br J Nutr. 88(6):587–605.

Funel C, Berrue F, Roussakis C, Rodriguez RF, Amade P. 2004. New cytotoxic steroids from the Indian Ocean sponge *Axinella cf. bidderi*. J Nat Prod. 67(3):491–494.

Gilbert NC, Rui Z, Neau DB, Waight MT, Bartlett SG, Boeglin WE, Brash AR, Newcomer ME. 2012. Conversion of human 5-lipoxygenase to a 15-lipoxygenase by a point mutation to mimic phosphorylation at Serine-663. Faseb J. 26(8):3222–3229.

Grille S, Zaslawski A, Thiele S, Plat J, Warnecke D. 2010. The functions of steryl glycosides come to those who wait: recent advances in plants, fungi, bacteria and animals. Prog Lipid Res. 49(3):262–288.

Ivanchina NV, Kicha AA, Stonik VA. 2011. Steroid glycosides from marine organisms. Steroids. 76(5):425–454.

Krishnan S, Chakraborty K, Joy M. 2020. First report of anti-inflammatory chromenyl derivatives from the spineless cuttlefish *Sepiella inermis*. Nat Prod Res. 34(17):2437–2447.

Krishnan S, Chakraborty K. 2019. Functional properties of ethyl acetate-methanol extract of commonly edible molluscs. J Aquat Food Prod T. 28(7):729–742.

Larsen LN, Dahl E, Bremer J. 1996. Peroxidative oxidation of leucodichloroluorescein by prostaglandin H synthase in prostaglandin biosynthesis from polyunsaturated fatty acids. Biochim Biophys Acta. 1299(1):47–53.

Lee YJ, Han S, Kim SH, Lee HS, Shin HJ, Lee JS, Lee J. 2017. Three new cytotoxic steroidal glycosides isolated from *Conus pulicarius* collected in Kosrae, Micronesia. Mar Drugs. 15(12):379.

Lipinski C, Hopkins A. 2004. Navigating chemical space for biology and medicine. Nature. 432(7019):855–861.

Makarieva TN, Stonik VA, Kapustina II, Boguslavsky VM, Dmitrenoik AS, Kalinin VI, Cordeiro ML, Djerassi C. 1993. Biosynthetic studies of marine lipids. 42. Biosynthesis of steroid and triterpenoid metabolites in the sea cucumber *Eupentacta fraudatrix*. Steroids. 58(11):508–517.

Maneesh A, Chakraborty K. 2017. Unprecedented antioxidative and anti-inflammatory aryl polyketides from the brown seaweed *Sargassum wightii*. Food Res Int. 100(Pt 1):640–649.

Mitome H, Shinohara M, Miyaoka H, Yamada Y. 2003. Synthesis and anti-tumor activity of new steroidal nuclear analogues of aragusterol A. Chem Pharm Bull (Tokyo). 51(6):640–645.

Nichols PD, Virtue P, Mooney BD, Elliott NG, Yearsley GK. 1998. Seafood the good food: the oil (fat) content and composition of Australian commercial fishes, shellfshes and crustaceans. Hobart: CSIRO Division of Marine Research and Deakin, A.C.T. Fisheries Research & Development Corporation (FRDC), Australia.

Ngoc NT, Huong PT, Thanh NV, Chi NT, Dang NH, Cuong NX, Nam NH, Thung DC, Kiem PV, Minh CV. 2017. Cytotoxic steroids from the Vietnamese soft coral *Sinularia conferta*. Chem Pharm Bull (Tokyo). 65(3):300–305.

Norman MD, Finn JK, Hochberg FG. 2014. Family Octopodidae. pp. 36–215. In: Jereb P, Roper CFE, Norman MD, Finn JK, editors. Cephalopods of the world. An annotated and illustrated catalogue of cephalopod species known to date. Vol. 3. Octopods and vampire squids. FAO Species Catalogue for Fishery Purposes, No. 4, Rome: FAO; 4(3):353 pp.

Pati P, Sahu BK, Panigrahy RC. 2015. Marine molluscs as a potential drug cabinet: an overview. Indian J Mar Sci. 44(7):961–970.

Paulose SK, Chakraborty K. 2021. Cistobislactones A-B, two sixteen-membered spiro-linked macrocylicbislactones from marine octopus *Cistopus indicus*: new anti-inflammatory agents attenuate arachidonate 5-lipoxygenase. Med Chem Res. 30:2042–2054.

Paulose SK, Chakraborty K. 2022. Cistobislactone, an undescribed variant of 14-membered bislactonic macrodiolide, from old-lady octopus *Cistopus indicus* (family Octopodidae) attenuates inflammatory lipoxygenase. Nat Prod Res. 36(12):3002–3012.

Salas S, Chakraborty K. 2018. First report of bioactive sterols from the muricid gastropod *Chicoreus ramosus*. Steroids. 137:57–63.

Vien LT, Ngoan BT, Hanh TT, Vinh LB, Thung DC, Thao DT, Thanh NV, Cuong NX, Nam NH, Kiem PV, et al. 2017. Steroid glycosides from the starfish *Pentaceraster gracilis*. J Asian Nat Prod Res. 19(5):474–480.

Wojdylo A, Oszmianski J, Czemerys R. 2007. Antioxidant activity and phenolic compounds in 32 selected herbs. Food Chem. 105(3):940–949.